Inorg. Chem. **2004**, *43*, 5112–5119

Ruthenium(II) Dipyridoquinoxaline-Norbornene: Synthesis, Properties, Crystal Structure, and Use as a ROMP Monomer

Ali Rezvani, Hassan S. Bazzi, Bingzhi Chen, Felaniaina Rakotondradany, and Hanadi F. Sleiman*

Department of Chemistry, McGill University, 801 Sherbrooke Street West, Montreal, QC, H3A 2K6 Canada

Received February 6, 2004

The synthesis, X-ray structure, and electrochemical and photophysical characterization of $[Ru(phen)_2dpq\text{-}n][PF_6]_2$ (phen = phenanthroline, dpq-n = dipyridoquinoxaline-norbornene) are described. This complex contains a $Ru(phen)_3^{2+}$ moiety in close conjugation with a norbornene unit and is the first example of a Ru(II) diimine complex capable of undergoing ring-opening metathesis polymerization. Luminescence studies of this complex showed an increase in quantum efficiency in polar solvents and in water. Preliminary ring-opening metathesis polymerization studies, carried out at low monomer-to-initiator ratio, showed the formation of an oligomeric mixture composed mainly of the dimer of this complex. This dimer exhibits photophysical and redox properties similar to those of the monomer, indicating that the $Ru(phen)_3^{2+}$ moiety remains intact during the polymerization.

Introduction

Ring-opening metathesis polymerization (ROMP) has recently played a major role in the controlled construction of functional polymers.[1] Because of its living nature[2] and its remarkable functional group tolerance, this reaction is especially amenable to the synthesis of polymers containing a well-defined arrangement of photoactive[3] and redox-active[4] units. A particularly interesting class of chromophores for incorporation into ROMP polymers are ruthenium(II) bipyridyl or phenanthroline complexes.[5] Because of their unique photophysical and redox properties, these molecules have been extensively investigated as components of light-harvesting assemblies and photochemically driven molecular devices, as well as photocatalysts and biological probes.[6−9] For these applications, binuclear and multinuclear assemblies containing Ru(II) diimine complexes are typically constructed in stepwise syntheses,[10] which can be time-consuming. On the other hand, the ROMP reaction of Ru(II) polypyridyl-containing monomers could result in more straightforward generation of multichromophoric polymers and block copolymers in a living fashion, with controlled molecular weights and narrow molecular weight distributions.[1,11] A number of polymeric systems containing Ru(II) diimines have been generated.[12] Free-radical polymerization[12a−d] and, more recently, anionic polymerization[12e−i] have been used

* To whom correspondence should be addressed. E-mail: hanadi.sleiman@mcgill.ca.

(1) Grubbs, R. H.; Tumas, W. *Science* **1989**, *243*, 907−915. Buchmeiser, M. R. *Chem. Rev.* **2000**, *100*, 1565−1604.
(2) Scholl, M.; Ding, S.; Lee, C. W.; Grubbs, R. H. *Org. Lett.* **1999**, *1* (6), 953−956. Schwab, P. E.; Grubbs, R. H.; Ziller, J. W. *J. Am. Chem. Soc.* **1996**, *118*, 100−110. Schwab, P.; France, M. B.; Ziller, J. W.; Grubbs, R. H. *Angew. Chem., Int. Ed. Engl.* **1995**, *34*, 2039−2041.
(3) Watkins, D. M.; Anne Fox, M. *J. Am. Chem. Soc.* **1996**, *118*, 4344−4353. (b) Zaami, N.; Slugovc, C.; Pogantsch, A.; Stelzer, F. *Macromol. Chem. Phys.* **2004**, *205*, 523−529.
(4) Nguyen, P.; Stojcevic, G.; Kulbaba, K.; MacLachlan, M. J.; Liu, X., H.; Lough, A. J.; Manners, I. *Macromolecules* **1998**, *31*, 5977−5983.
(5) Juris, A.; Balzani, V.; Barigelletti, F.; Campagna, S.; Belser, P.; Von Zelewsky, A. *Coord. Chem. Rev.* **1988**, *84*, 85−277.
(6) Loiseau, F.; Marzanni, G.; Quici, S.; Indelli, M. T.; Campagna, S. *Chem. Commun.* **2003**, 286−287.
(7) Ballardini, R.; Balzani, V.; Credi, A.; Gandolfi, M. T.; Venturi, M. *Acc. Chem. Res.* **2001**, *34*, 445−455.
(8) Suzuki, M.; Kimura, M.; Hanabusa, K.; Shirai, H. *Macromol. Chem. Phys.* **1998**, *199*, 945−948. (b) Levy, B. *J. Electroceram.* **1997**, *1*, 239−272. (c) Nageswara Rao, N. *J. Mol. Catal.* **1994**, *93*, 23−7.
(9) Nunez, M. E.; Barton, J. K. *Curr. Opin. Chem. Biol.* **2000**, *4*, 199. (b) Boon, E, M.; Barton, J. K. *Curr. Opin. Struct. Biol.* **2002**, *12*, 320.
(10) Kaes, C.; Katz, A.; Hosseini, M. W. *Chem. Rev.* **2000**, *100*, 3553−3590. Chiorboli, C.; Rodgers, M. A. J.; Scandola, F. *J. Am. Chem. Soc.* **2003**, *125*, 483−491.
(11) Bazzi, H. S.; Sleiman, H. F. *Macromolecules* **2002**, *35*, 624−629.
(12) Card, R. J.; Neckers, D. C. *Inorg. Chem.* **1978**, *17*, 2345−2349. (b) Olmsted, J., III; McClanahan, S. F.; Danielson, E.; Younathan, J. N.; Meyer, T. J. *J. Am. Chem. Soc.* **1987**, *109*, 3297−3301. (c) Strouse, G. F.; Worl, L. A.; Younathan, J. N.; Meyer, T. J. *J. Am. Chem. Soc.* **1989**, *111*, 9101−9102. (d) Jones, W. E.; Baxter, S. M.; Strouse, G. F.; Meyer, T. J. *J. Am. Chem. Soc.* **1993**, *111*, 7363−7373. (e) Dupray, L. N.; Meyer, T. J. *Inorg. Chem.* **1996**, *35*, 6299−6307. (f) Leasure, R. M.; Kajita, T.; Meyer, T. J. *Inorg. Chem.* **1996**, *35*, 5962−5963. (g) Friesen, D. A.; Kajita, T.; Danielson, E.; Meyer, T. J. *Inorg. Chem.* **1998**, *37*, 2756−2762. (h) Fleming, C. N.; Maxwell, K. A.; DeSimone, J. M.; Meyer, T. J.; Papanikolas, J. M. *J. Am. Chem. Soc.* **2001**, *123*, 10336−10347. (i) Fleming, C. N.; Dupray, L. M.; Papanikolas, J. M.; Meyer, T. J. *J. Phys. Chem. A* **2002**, *106*, 2328−2334.

10.1021/ic0498438 CCC: $27.50
Published on Web 07/13/2004

Scheme 1

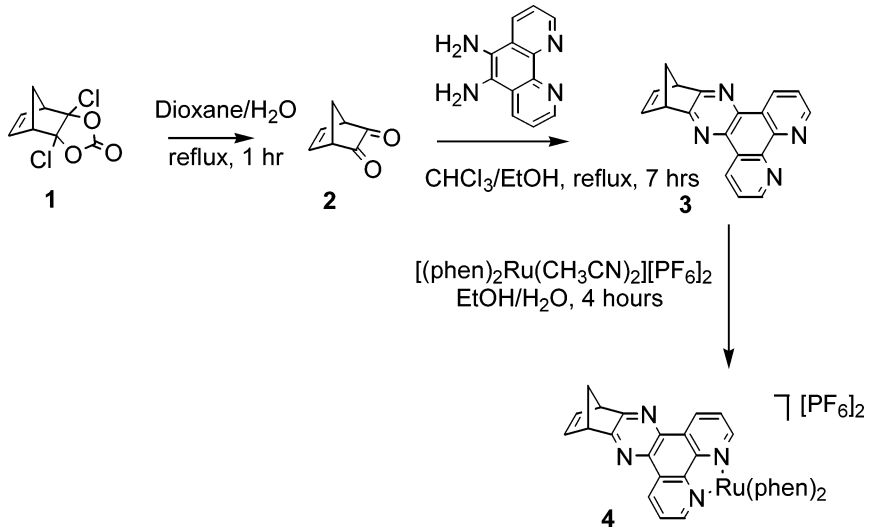

Scheme 2

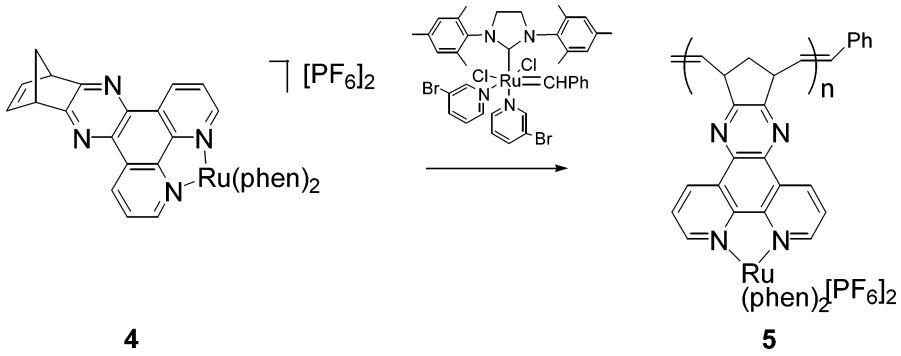

to synthesize precursors that were converted to Ru(bpy)$_3^{2+}$-containing homopolymers. These studies have shed light on novel mechanisms of photoinduced energy transfer in these polymers.[12] Star[13a] and block copolymers[13b] containing a Ru(II) bipyridine or terpyridine core and polymer arms have been constructed. Conjugated polymers containing Ru(II) polypyridyl complexes have also been synthesized via step polymerization mechanisms[14] and have been investigated as redox-active,[14a] metal-ion sensing,[14b−d] photoconductive,[14e] photocatalytic,[14f] and photorefractive[14g] materials. However, there are no previous examples of the use of living polymerization, such as ROMP, to directly generate ruthenium(II) diimine-containing polymers.

We here report the synthesis of dipyridoquinoxaline-norbornene ligand **3** and its conversion to the first Ru(phen)$_3^{2+}$-containing ROMP monomer **4** (Scheme 1). The Ru(II) dipyridoquinoxaline moiety in complex **4** and related Ru(II) dipyridophenazine complexes have been extensively investigated for their photophysical properties and DNA binding ability.[9,15] The synthesis and X-ray structure of monomer **4** as well as its electrochemical and photophysical characterization are described. Preliminary studies show that monomer **4** can undergo ring-opening metathesis polymerization to yield an oligomer containing luminescent and redox-active Ru(phen)$_3^{2+}$ in its repeat units (Scheme 2).

(13) Smith, A. P.; Fraser, C. L. *Macromolecules* **2003**, *36*, 5520−5525. (b) Lohmeijer, B. G. G.; Schubert, U. S. *Angew. Chem., Int. Ed.* **2002**, *41*, 3825−3829.

Results and Discussion

Synthesis of Ligand 3 and Complex 4. The design of precursor **3** includes a norbornene unit, which can undergo controlled ring-opening metathesis polymerization,[1] as well

(14) Grosshenny, V.; Harriman, A.; Gisselbrecht, J.,-P.; Ziessel, R. *J. Am. Chem. Soc.* **1996**, *118*, 10315−10316. (b) Swager, T. M.; Zhu, S. S. *J. Am. Chem. Soc.* **1997**, *119*, 12568. (c) Wang, B.; Wasielewski, M. R. *J. Am. Chem. Soc.* **1997**, *119*, 12. (d) Kimura, M.; Horai, T.; Hanabusa, K.; Shirai, H. *Adv. Mater*. **1998**, *10*, 459. (e) Peng, Z.; Yu, L. *J. Am. Chem. Soc.* **1996**, *118*, 3777. (f) Yamamoto, T.; Maruyama, T.; Zhou, Z.,-H.; Ito, T. F. T.; Yoneda, Y.; Begum, F.; Ikeda, T.; Sasaki, S.; Takezoe, H.; Fukuda, A.; Kubota, K. *J. Am. Chem. Soc.* **1994**, *116*, 4832. (g) Peng, Z.; Gharavi, A. R.; Yu, L. *J. Am. Chem. Soc.* **1997**, *119*, 4622. (h) Yiting, L.; Whittle, C. E.; Walters, K. A.; Ley, K. D.; Schanze, K. S. *Pure Appl. Chem.* **2001**, *73*, 497−501. (i) Knapp, R.; Schott, A.; Rehahn, M. *Macromolecules* **1996**, *29*, 478−480. (j) Ley, K. D.; Whittle, C. E.; Bartberger, M. D.; Schanze, K. S. *J. Am. Chem. Soc.* **1997**, *119*, 3423−3424. (k) Liu, Y.; Li, Y.; Schanze, K. S. *J. Photochem. Photobiol. C.: Photochem. Rev.* **2002**, *3*, 1−23.

(15) The quinoxaline moiety in complex **4** is in direct conjugation with the norbornene unit. The result of this interaction is that the ROMP product of **4**, oligomer **5**, is potentially a precursor to a fully conjugated oligomer, which can be accessed by oxidation (dehydrogenation) of the norbornene backbone. (see ref 11). (a) Amouyal, E.; Homsi, A.; Chambron, J.-C.; Sauvage, J.-P. *J. Chem. Soc., Dalton Trans.* **1990**, 1841−1845. (b) Friedman, A. E.; Chambron, J. C.; Sauvage, J. P.; Turro, N. J.; Barton, J. K. *J. Am. Chem. Soc.* **1990**, *112*, 4960−4962. (c) Hartshorn, R. M.; Barton, J. K. *J. Am. Chem. Soc.* **1992**, *114*, 5919−5925. (d) Nair, R. B.; Cullum, B. M.; Murphy, C. J. *Inorg. Chem.* **1997**, *36*, 962−965. (e) Faust, R.; Ott, S. *J. Chem. Soc., Dalton Trans.* **2002**, 1946−1953. (f) Ambroise, A.; Maiya, B. G. *Inorg. Chem.* **2000**, *39*, 4264−4272. (g) Gulyas, P. T.; Smith, T. A.; Paddon-Row, N. *J. Chem. Soc., Dalton Trans.* **1999**, 1325−1335 and references therein. (h) Brennaman, M. K.; Alstrum-Acevedo, J. H.; Fleming, C. N.; Jang, P.; Meyer, T. J.; Papanikolas, J. M. *J. Am. Chem. Soc.* **2002**, *124*, 15084−15098 and references therein.

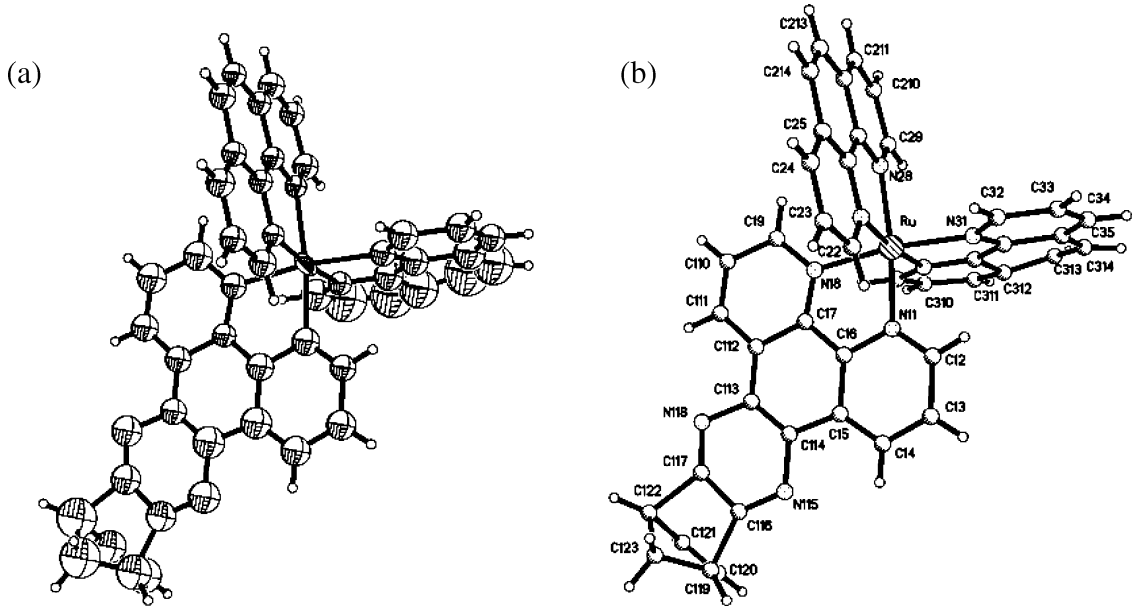

Figure 1. (a) ORTEP drawing of the cation of complex **4**; ellipsoids are drawn at 30% probability level and hydrogens are represented by spheres of arbitrary size. (b) Atom-numbering scheme.

as a phenanthroline unit for metal complexation. Of particular importance is the intimate coupling of the norbornene and the metal-binding unit via a conjugated quinoxaline moiety (Scheme 1).[15] Compound **1**, containing a dichlorocarbonate functionality, is a convenient precursor to a 1,2-diketone and was used as the starting material.[16] **1** was readily hydrolyzed to the norbornene dione **2** by treatment with refluxing dioxane/H_2O (1:2). The resulting dione was subsequently treated with 5,6-diamino-1,10-phenanthroline[17] in refluxing chloroform/ethanol (1:5), to yield norbornene phenanthroline ligand **3**. Compound **3** was characterized by ^{1}H NMR, ^{13}C NMR, UV/vis, and fluorescence spectroscopies and high-resolution FAB-MS.

Because of its strongly metal-coordinating phenanthroline ligand and the possibility of binding this unit to the ROMP catalyst, compound **3** was not directly used as a monomer in ROMP reactions. Instead, metal complexation of **3** was carried out (Scheme 1). Of concern was the possibility that the metal complexes would bind the norbornene π-bond, instead of the phenanthroline unit in **3**. Upon treatment of **3** with $[(phen)_2Ru(CH_3CN)_2][PF_6]_2$[18] in refluxing ethanol/water (1:1), complex **4** was obtained as a yellow-orange solid and was characterized by ^{1}H NMR and ^{13}C NMR spectroscopies, ESI-MS, high-resolution FAB-MS, and X-ray crystallography. These methods show that the $Ru(phen)_2^{2+}$ is indeed coordinated to the phenanthroline unit in **4**. Similarly, reaction of ligand **3** with K_2PtCl_4 results in the efficient formation of the complex Cl_2Pt(**3**), where the platinum(II) center is coordinated to the phenanthroline moiety in **3**.[19]

Table 1. Selected Bonds Lengths (Å) and Angles (deg) for Monomer **4**

Ru−N(11)	2.02(2)	Ru−N(18)	2.06(2)
Ru−N(38)	2.02(2)	Ru−N(28)	2.08(2)
Ru−N(21)	2.03(2)	Ru−N(31)	2.04(2)
C(17)−C(16)	1.40(2)	C(17)−C(112)	1.45(3)
C(15)−C(16)	1.45(3)	C(15)−C(114)	1.45(3)
C(114)−C(113)	1.34(3)	C(113)−C(112)	1.38(3)
C(114)− N(115)	1.42(4)	C(116)−N(115)	1.33(4)
C(113)−N(118)	1.42(4)	C(117)− N(118)	1.27(4)
C(116)−C(117)	1.42(5)	C(122)−C(117)	1.73(6)
C(116)−C(119)	1.60(5)	C(122)−C(121)	1.54(5)
C(119)−C(120)	1.58(5)	C(121)−C(120)	1.27(5)
C(119)−C(123)	1.44(5)	C(122)−C(123)	1.59(6)

N(31)−Ru−N(38)	78.3(9)	N(11)−Ru−N(18)	78.6(9)
N(28)−Ru−N(21)	77.4(8)	N(115)−C(114)−C(15)	113(3)
N(115)−C(114)−C(113)	124(3)	N(118)−C(113)−C(112)	114(3)
N(118)−C(113)−C(114)	122(3)	N(115)−C(116)−C(117)	115(4)
N(118)−C(117)−C(116)	133(5)	N(115)−C(116)−C(119)	135(4)
N(118)−C(117)−C(122)	125(4)	C(113)−N(118)−C(117)	110(3)
C(114)−N(115)−C(116)	116(4)	C(117)−C(116)−C(119)	109(4)
C(116)−C(117)−C(122)	102(4)	C(116)−C(119)−C(123)	100(4)
C(117)−C(122)−C(123)	93(4)	C(122)−C(121)−C(120)	118(5)
C(119)−C(120)−C(121)	101(5)	C(123)−C(119)−C(120)	109(4)
C(123)−C(122)−C(121)	97(4)	C(117)−C(122)−C(121)	95(4)
C(116)−C(119)−C(120)	93(3)		

Thus, ligand **3** can act as a convenient precursor for metal−phenanthroline-containing ROMP monomers.

Crystal Structure of 4. Single crystals of **4** were grown by vapor diffusion of ether into a dichloromethane solution of this complex. The X-ray crystallographic investigation of **4** consists of a $(phen)_2Ru$(dipyridoquinoxaline-norbornene)$^{2+}$ cation with two PF_6^- anions (one anion is disordered). An ORTEP drawing of the cation is shown in Figure 1. Selected bond lengths and angles are summarized in Table 1.

As shown in Figure 1, the ruthenium center is chelated to two phenanthroline ligands oriented in a cis geometry and to a dipyridoquinoxaline-norbornene ligand. The coordination geometry around the ruthenium is a distorted octahedron, with bite angles of 77−78° for all three bidentate ligands. The Ru−N bond lengths are in the normal range for all three ligands (2.03−2.08 Å).[20] The dipyridoquinoxaline portion

(16) Scharf, H.-D.; Küsters, W. *Chem. Ber.* **1972**, *105*, 564−574. Scharf, H.-D.; Pinske, W.; Feilen, M.-H.; Droste, W. *Chem. Ber.* **1972**, *105*, 554−563.
(17) Bodige, S.; MacDonnell, F. M. *Tetrahedron Lett.* **1997**, *38*, 8159−8160.
(18) Brown, G. M.; Callahan, R. W.; Meyer, T. J. *Inorg. Chem.* **1975**, *14*, 1915−1921.
(19) Rezvani, A.; Sleiman, H. F. McGill University, Montreal, Canada, unpublished results.

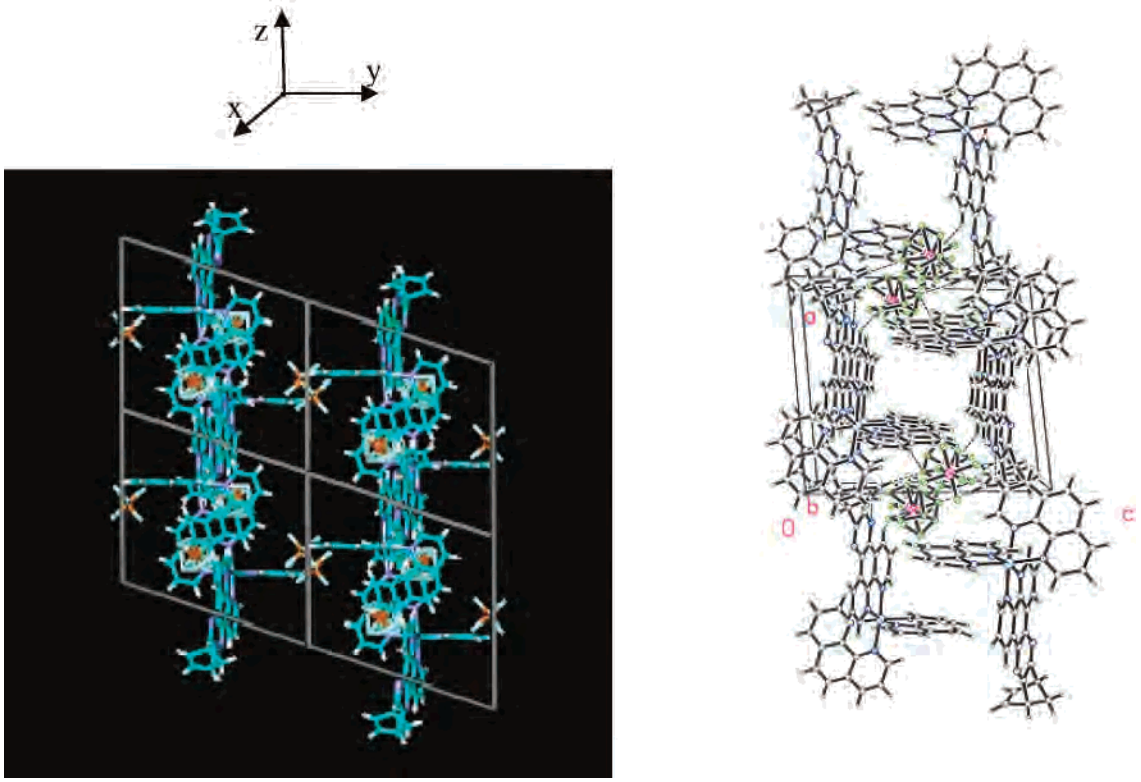

Figure 2. Side view of the stacking interactions in complex **4**, showing one layer (left) and multiple layers (right) along the *x* axis.

of the molecule is essentially planar. The pyrazine ring is significantly distorted, with the N−C bonds to the norbornene unit shorter (N118−C-117 = 1.27 Å, N115−C116 = 1.33 Å) than the N−C bonds to the phenanthroline unit (N118−C113 = 1.42 Å, N115−C114 = 1.42 Å). This double-bond localization in the pyrazine ring might indicate reduced electronic communication between the phenanthroline portion of the molecule and the norbornene-diimine unit. The norbornene portion also shows some distortion relative to other norbornene systems.[21] Although the C=C double bond length is normal within experimental error, the ring appears to be unsymmetrical, with longer bonds and wider angles on one side of the single bridgehead carbon than on the other side (C116−C119 = 1.6 Å, C117−C122 = 1.73 Å and C121−C120−C119 = 101°, C120−C121−C122 = 118°).

X-ray structural studies show that complex **4** exhibits a highly ordered packing arrangement, shown in Figure 2. Neighboring molecules along the *x* axis show π-stacking of their phenanthroline units, as well as head-to-tail stacking of their dipyridoquinoxaline-norbornene moieties. The unit cell consists of stacks of the two enantiomers of complex **4**. Interestingly, these phenanthroline and dipyridoquinoxaline stacks form small, semirectangular cavities lined with two dipyridoquinoxaline stacks (distance ca. 8 Å) on one side and two phenanthroline-PF_6^--phenanthroline stacks (distance between the phenanthrolines ca. 13 Å) on the other side.

(20) Zou, X.-H.; Li, H.; Yang, G.; Deng, H.; Liu, J.; Li, R.-H.; Zhang, Q.-L.; Xiong, Y.; Ji, L.-N. *Inorg. Chem.* **2001**, *40*, 7091−7095. Note that the relatively large *R* value for this structure is due to the fact that the examined crystal is very small (0.05 × 0.05 × 0.18 mm), resulting in fewer observed reflections than necessary for a full refinement.

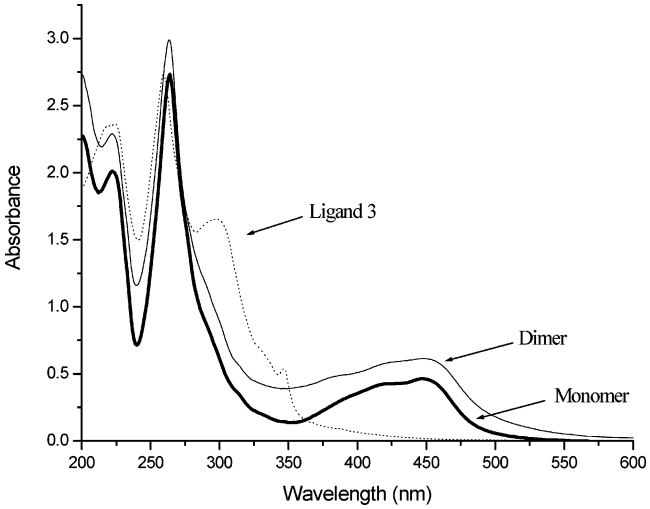

Figure 3. UV/vis absorption spectra of ligand **3**, monomer **4**, and dimer **6**.

Absorption and Emission Spectra. UV/vis absorption spectra of ligand **3** were measured in CH_3CN and showed bands at 259 and 299 nm, as well as a shoulder at 347 nm (Figure 3). Excitation of **3** in acetonitrile at 250 nm results in a broad emission band centered at 390 nm. Upon coordination to Ru(phen)$_2^{2+}$, the UV/vis absorbance spectrum of **4** in CH_3CN shows two broad bands at 413 and 444 nm, assigned to Ru(II) dπ−π* metal-to-ligand charge transfer (MLCT) transitions (Figure 3). In addition, more intense bands at 235 and 275 nm were assigned to ligand-centered π−π* transitions. These values and assignments are con-

(21) Macdonald, A. C.; Trotter, J. *Acta Crystallogr*. **1965**, *19*, 456−463.

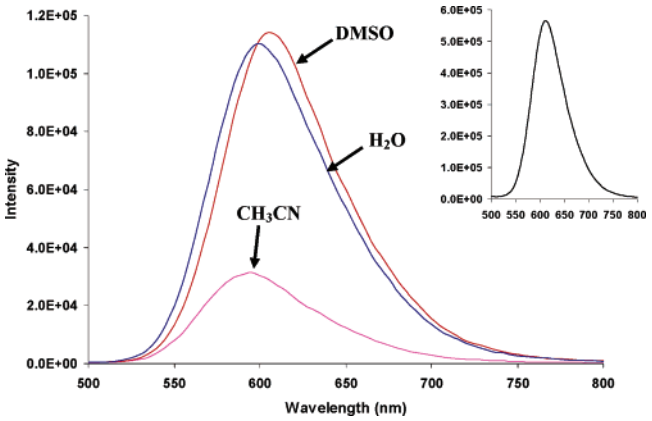

Figure 4. Emission spectra of complex **4** in different solvents and of dimer **6** (inset).

Table 2. Emission Data of Complex **4** in Different Solvents and in Air (T = 298 K)

solvent	λ_{max}^{em} (nm)	quantum yield[a] (in air)
CH_2Cl_2	575	0.015
CH_3CN	593	0.011
MeOH	600	0.014
DMF	602	0.024
DMSO	605	0.052
water	603	0.043

[a] Relative quantum yields were compared to $Ru(bpy)_3^{2+}$ in aerated water (Φ = 0.028).

sistent with those of a number of related complexes in the literature.[9,15]

Complex **4** contains a $[(phen)_2Ru(dipyridoquinoxaline)]^{2+}$ unit, which is structurally related to $[(phen)_2Ru(dppz)]^{2+}$ (dppz = dipyridophenazine).[15] The latter has been extensively investigated as a "molecular light switch" whose emission is undetectable in water but is readily turned back "on" in aprotic solvents, as well as in the presence of DNA and micellar particles.[15] We were thus interested in investigating the luminescence properties of complex **4** and their solvent dependence, to evaluate the sensitivity of this molecule to its environment. Steady-state emission spectra were recorded for **4** in acetonitrile and showed a strong luminescence at 595 nm upon excitation of the MLCT band at 420 nm. This value is hypsochromically shifted from the emission wavelength of $[Ru(phen)_2(dppz)]^{2+}$ (618 nm),[15b] consistent with the stabilization of the ^{3}MLCT state in the latter complex by the more π-accepting dppz, which contains an additional fused benzene ring compared to dipyridoquinoxaline. Figure 4 shows the emission spectra of complex **4** in a number of solvents, and Table 2 lists its luminescence wavelengths and quantum yields in these solvents. The emission wavelength was found to increase with increasing solvent polarity, likely due to the stabilization of the MLCT state with polar solvents. Interestingly, the emission intensity of **4** *increases* with increasing solvent polarity and shows an enhancement in water.

This behavior is different from most previously studied Ru(II)-dppz and Ru(II)-dipyridoquinoxaline complexes, which usually show lower emission quantum yields in polar solvents, as well as quenching effects in water.[15] Although we cannot presently explain this luminescence enhancement

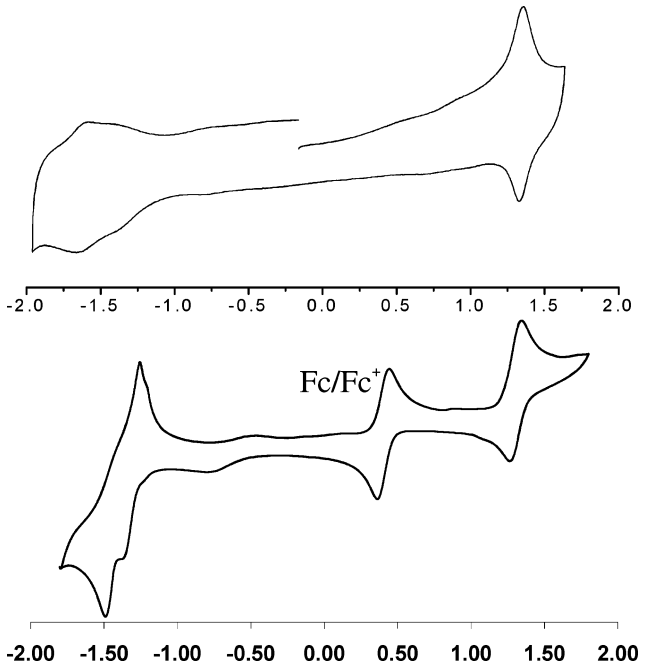

Figure 5. Cyclic voltammograms of complex **4** (below) and dimer **6** (above).

in water and polar solvents, these results indicate that the nature of the luminescent MLCT state in complex **4** is possibly different from the dual MLCT nature of the $[(phen)_2Ru(dppz)]^{2+}$ complex (a "bright" state associated with charge transfer from Ru(II) to the bipyridine fragment and a "dark" state associated with charge transfer to the phenazine portion of the dppz).[15h] As previously mentioned, X-ray crystallographic data of **4** show reduced electronic delocalization in the pyrazine ring, and thus the emissive MLCT state in **4** might be more localized on the phenanthroline portion of the dipyridoquinoxaline ligand than on its pyrazine portion.

Electrochemical Studies. Cyclic voltammetry was recorded on a solution of complex **4** in CH_3CN, using tetrabutylammonium hexafluorophosphate as the electrolyte (Figure 5). A quasireversible oxidation couple at 1.31 V vs NHE occurred in the range typical of $Ru^{3+/2+}$ couples[15g] and was assigned as a Ru(II)-based oxidation. The reversibility of this peak was confirmed by its constant half-potential as the scan rate was changed from 50 to 500 mV/s. Two reduction couples, at −1.25 and −1.46 V, were observed and assigned to the reduction of the ligands on ruthenium (the dipyridoquinoxaline and the phenanthrolines). The formal half-potential of the first reduction process (−1.25 V) of **4** is more negative than that of $[(bpy)_2Ru(dppz)]^{2+}$ (−0.97 V),[15a] whose first reduction is thought to reside on the dppz ligand, and more positive than that of $[Ru(phen)_3]^{2+}$ (−1.36 V).[15g] These results are consistent with the first reduction of **4** residing on the dipyridoquinoxaline ligand, whose π-accepting ability is expected to be greater than that of phenanthroline but lower than that of dppz.[23]

Ring-Opening Metathesis Polymerization of 4. The ring-opening metathesis polymerization of complex **4** was examined using the ruthenium alkylidene $[(H_2IMes)(3\text{-Br-py})_2(Cl)_2Ru{=}CHPh]$.[23] This ruthenium catalyst has

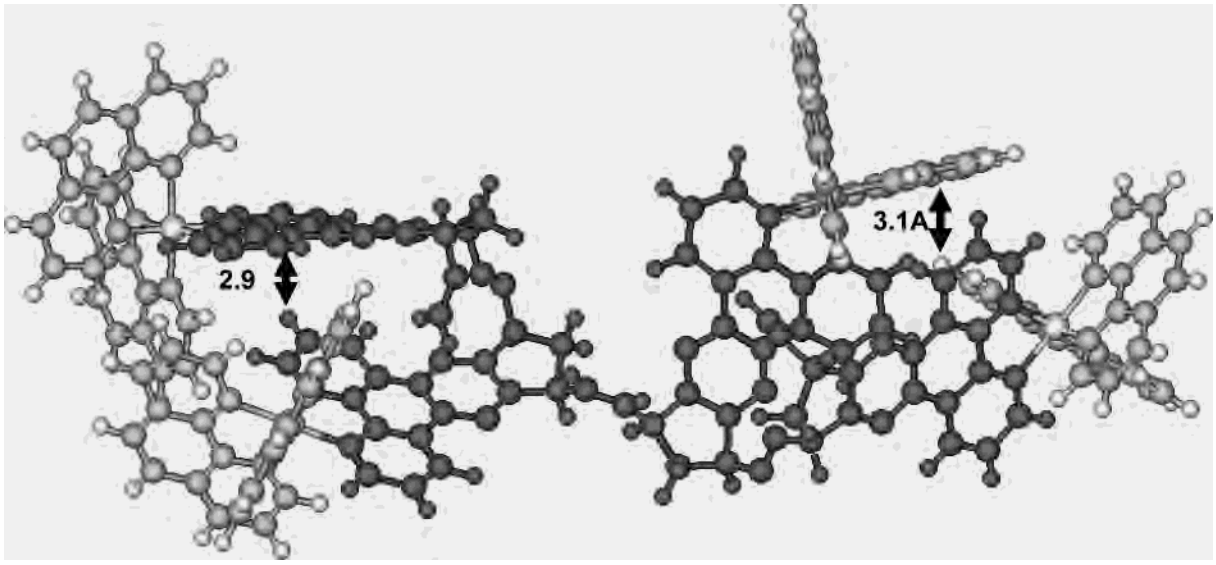

Figure 6. Optimized structure (MM+) of oligomer **5**, calculated from the crystal structure of **4**. The ROMP oligomer backbone is shown in dark gray, and the Ru(phen)$_2^{2+}$units are shown in light gray.

been shown to have high ROMP activity, due to coordination to the electron-rich N-heterocyclic carbene ligand, as well as fast initiation due to the labile 3-bromopyridine ligands.[23] The catalyst was added to a stirring solution of complex **4** (2 equiv) in CH_2Cl_2. After 12 h, the reaction was quenched with ethyl vinyl ether, and the product was collected by precipitation into hexanes and purified by preparative size-exclusion chromatography. Thin layer chromatographic analysis (alumina, 95:5 mixture of acetone/NH_4PF_6(aq)) showed the absence of monomer **4** in the product.

Mass spectrometry was used to identify the resulting oligomer **5**. Matrix-assisted laser desorption ionization time-of-flight mass spectrometry (MALDI-TOF/MS) showed that a mixture of oligomers (dimer to pentamer) was produced. The composition of the oligomeric product was further determined by electrospray ionization MS (EI/MS), which showed the dimer of **4** (complex **6**) as the major product. Isotopically resolved signals centered at m/z = 595.1 and 965.1 correspond to (**6** − 3PF_6 + H_2O)$^{3+}$ and (**6** − 2PF_6 + H_2O)$^{2+}$ species, respectively, resulting from the loss of the corresponding number of counterions and association with one molecule of water.[24] These signals are in very good agreement with the theoretical isotopic distribution of the predicted elemental composition of the above two dimeric species at m/z = 594.44 and 964.15.[24] Oligomer **5** was further purified by size-exclusion chromatography, using toluene/acetonitrile (3:1) as the eluent. The second orange band was isolated, and its MALDI-TOF spectrum showed the exclusive presence of dimer **6** and the absence of any higher-order oligomers. Electrospray mass spectrometry of this complex showed isotopically resolved signals at m/z =584 (**6** −3 PF_6 − [CH_2 end group])$^{3+}$, 948 (**6** − 2PF_6 − [CH_2])$^{2+}$, and 966 (**6** − 2PF_6 + H_2O)$^{2+}$.[24,25] UV/vis spectrometry of dimer **6** showed absorbance properties similar to those of complex **4**, indicating that the ruthenium moiety, along with its ligands, remained intact during the polymerization (Figure 3). Steady-state emission spectra of dimer **6** showed a strong emission at 610 nm, upon excitation at 430 nm in acetonitrile (Figure 4, inset). Cyclic voltammetry of dimer **6** (Figure 5) gave a single $Ru^{2+/3+}$ oxidation peak with a half-wave oxidation potential of 1.35 V, which is only slightly different from the monomer $Ru^{2+/3+}$ potential. The presence of a single oxidation peak suggests weak electronic communication between the two ruthenium centers in dimer **6**.[26] Two bands were observed at negative potentials (−1.38 and −1.62 V) and are likely the result of ligand-centered reduction processes of dimer **6**.

To further investigate the expected structure of oligomer **5**, molecular modeling studies were carried out on the tetramer (**5**, n = 4), using crystal parameters of monomer **4** (MM+, conjugate gradient method, rms gradient 10^{-5}, Hyperchem 5.01). The optimized structure of this tetramer shows a folded quasihelical arrangement, where two adjacent monomeric units interact through edge-to-face contacts (Figure 6). Despite the close arrangement of adjacent

(22) It is of note that the luminescence intensities of Ru(phen)$_3^{2+}$ and Ru(bpy)$_3^{2+}$ are suppressed in water, thus ruling out the assignment of the emissive MLCT band in **4** as phenanthroline-centered. (a) Durham, B.; Caspar, J. V.; Nagle, J. K.; Meyer, T. J. *J. Am. Chem. Soc.* **1982**, *104*, 4803−4810. (b) Caspar, J. V.; Meyer, T. J. *J. Am. Chem. Soc.* **1983**, *105*, 5, 5583−5590. (c) Hartmann, P.; Leiner, M. J. P.; Draxler, S.; Lippitsch, M. E. *Chem. Phys.* **1996**, *207*, 137−146.

(23) Using the first-generation Grubbs catalyst $Cl_2(PCy_3)_2Ru$=CHPh for the ROMP of **4** gave some oligomer, but with lower yields than using the more active third-generation Grubbs catalyst. (a) Love, J. A.; Morgan, J. P.; Trnka, T. M.; Grubbs, R. H. *Angew. Chem., Int. Ed.* **2002**, *41*, 4035−4037. (b) Choi, T.-L.; Grubbs, R. H. *Angew. Chem., Int. Ed.* **2003**, *42*, 1743−1746.

(24) See Supporting Information.

(25) The ^{1}H NMR spectrum of dimer **6** showed the correct number of aliphatic, olefinic, and aromatic peaks, with an unusual downfield shift of both the olefin and bridgehead peaks upon dimerization. This possibly suggests the existence of tautomers of dimer **6** with unsaturation in the norbornene ring (see Supporting Information).

(26) The potentials of the anodic and cathodic peaks for the $Ru^{2+/3+}$ couple in dimer **6** are close in value (1.34/1.36 V). This might possibly indicate that the species is partially adsorbed onto the electrode. This phenomenon has been observed for other Ru-containing oligomers and might be due to the irreversible adsorption of some twice-reduced ruthenium onto the electrode. Abruna, H. D.; Teng, A. Y.; Samuel, G. J.; Meyer, T. J. *J. Am. Chem. Soc.* **1979**, *101*, 6745.

Ru(II) units, our molecular modeling studies predict no significant steric or energetic barriers to the formation of oligomer **5**. The above results thus indicate that complex **4** can be successfully used in ring-opening metathesis reactions to generate Ru(II)-containing oligomers.

Conclusions

We have shown the synthesis of the first Ru(II) phenanthroline-containing monomer **4**, capable of undergoing ring-opening metathesis polymerization. This molecule contains a $(phen)_2Ru^{2+}$ center coordinated to a dipyridoquinoxaline-norbornene unit, with intimate electronic coupling of its phenanthroline and norbornene portions. The crystal structure and electrochemical and photophysical characterization of complex **4** are described. Of note is the luminescence enhancement of **4** in polar solvents and in water, which differs from the behavior of most previously described Ru(II) dipyridophenazine or dipyridoquinoxaline complexes and might be an indication of a different nature of the emissive MLCT state in this complex. Preliminary ring-opening metathesis polymerization studies, carried out at low monomer-to-initiator ratio (2:1), showed the formation of an oligomeric mixture **5** composed mainly of the ROMP dimer of **4** (complex **6**). Dimer **6** exhibits photophysical properties similar to those of complex **4**, indicating that the Ru(II) moiety remained intact in the ROMP reaction, and its cyclic voltammogram indicates weak electronic communication between the ruthenium centers. We are currently investigating the properties of the ROMP polymers of **4** in further detail and generating these from enantiomerically pure monomers. In addition, we are studying possible methods for the conversion of the polymer backbone in **5** to a conjugated form, in analogy with our previous studies on a similar system,[11] to create Ru(II)-containing conjugated polymers in a controlled manner.

Experimental Procedures

General Considerations. All reactions were carried out under a dry nitrogen atmosphere. ^{1}H NMR spectra were recorded on a Varian M400 spectrometer operated at 400.140 MHz and ^{13}C NMR on a Varian M300 spectrometer operated at 75.459 MHz. Chemical shifts are reported in ppm relative to the deuterated solvent resonances. UV/vis spectra were recorded on a Varian Cary 300 spectrophotometer. Fluorescence experiments were carried out on a PTI (Photon Technology International) TimeMaster model C-720F spectrofluorimeter. The emission spectra were recorded from 450 to 800 nm. The slit widths for both excitation and emission were set at 3 nm. Electrochemical experiments were performed using a Solatran 1255/1286-potentiostat/galvanostat. Three electrodes were utilized in this system: a platinum disk working electrode, a platinum wire auxiliary electrode, and a silver wire quasireference electrode. The platinum disk working electrode was manually cleaned with 1-μm diamond polish prior to each scan. Ferrocene (E° = 0.4 V relative to NHE) was used as an internal reference. The supporting electrolyte, 0.1 M tetrabutylammonium hexafluorophosphate (TBAH), was recrystallized twice from ethanol and vacuum-dried at 110° C overnight.

Molecular modeling studies were carried out by constructing a ring-opened structure of monomer **4** from its available crystal data. A dimer was created from this structure and was optimized using MM+ (Hyperchem 5.01), with an rms gradient of 10^{-5} (conjugate gradient method). Then, two dimers were covalently linked and optimized using the same method. The dihedral angle between the monomeric units was then deliberately altered so as to place these two units in a trans orientation, and optimization resulted in the same folded structure shown in Figure 6.

Materials. All reagents were purchased from Aldrich and used as received. Monomer **1**,[16] $Ru(phen)_2Cl_2$,[18] $[Ru(phen)_2(CH_3CN)_2](PF_6)_2$,[18] 5,6-diamino-1,10-phenanthroline,[17] and $[(H_2IMes)(3\text{-Br-py})_2(Cl)_2Ru{=}CHPh]$[23] were synthesized according to literature procedures. Acetonitrile (CH_3CN) and dichloromethane (CH_2Cl_2) were distilled from CaH_2. Solvents for cyclic voltammetry (acetonitrile and dimethylformamide) were distilled over alumina, degassed, and placed under argon prior to use. Deuterated solvents were purchased from Cambridge Isotope Laboratories and used without further purification.

Synthesis of the Norbornene Phenanthroline Ligand 3. In a round-bottom flask, *exo-cis*-2,3-dichloro-*endo-cis*-2,3-carbonatonorbornene (250 mg, 1.36 mmol) was dissolved in a mixture of 1,4-dioxane/water (1:2, 9 mL) with stirring. The mixture was then refluxed for 1 h, and the color of the solution became deep orange. The solution was cooled to room temperature and extracted with diethyl ether (100 mL). The organic phase was collected and dried over $MgSO_4$. The solvent was then removed under vacuum to afford a viscous yellowish liquid which was stored under nitrogen in the dark.

In a separate round-bottom flask wrapped with aluminum foil, 5,6-diamino-1,10-phenanthroline (210 mg, 1 mmol) was suspended in 25 mL of anhydrous ethanol, and the resulting mixture was brought to reflux. A chloroform solution of the yellowish norbornene dione prepared above (5 mL) was added dropwise using an addition funnel, and refluxing was continued overnight. The solution was cooled to room temperature, and the solvent was removed under vacuum. The resulting solid was dissolved in chloroform (40 mL) and filtered to remove unreacted 5,6-diamino-1,10-phenanthroline. Evaporation of the solvent and purification by chromatography (neutral alumina, 5% methanol in dichloromethane) gave a tan solid. Yield = 180 mg (60%). ^{1}H NMR δ (CD_2Cl_2): 9.36 (d, 2H), 9.11 (d, 2H), 7.72 (d, 2H), 7.00 (s, 2H), 4.09 (s, 2H), 2.85 (d, 1H), 2.75 (d, H). ^{13}C NMR δ (CD_2Cl_2): 170.01, 149.56, 143.89, 141.29, 136.16, 133.58, 128.25, 126.23, 65.96, 50.09. UV/vis: $\lambda_{max}(CH_3CN)$ = 224 nm, 259, 299, and 347 nm. HR−FAB MS: Theoretical calculated for $[C_{19}H_{12}N_4 + H^+]$, 297.1141; found, 297.1140.

Synthesis of Complex 4. $[Ru(phen)_2(CH_3CN)_2](PF_6)_2$ (340 mg, 0.4 mmol) and ligand **3** (157 mg, 0.53 mmol) were suspended in a 1:1 mixture of water and ethanol (60 mL), and the resulting solution was refluxed for 7 h. After evaporation of the solvent, the obtained solid was dissolved in 2 mL of CH_2Cl_2 and precipitated in diethyl ether to give an orange solid, which was filtered, washed with ether, and dried under vacuum. Chromatography (neutral alumina, 1:1 mixture of CH_3CN and toluene) yielded an orange-yellow solid. Yield = 260 mg (61%). ^{1}H NMR δ (CD_2Cl_2): 9.56 (d, 2H), 8.55 (d, 4H), 8.21 (s, 4H), 8.13 (d, 2H), 8.07 (m, 4H), 7.81 (m, 2H), 7.71 (m, 4H), 7.05 (s, 2H), 4.21 (s, 2H), 2.95 (d, 1H), 2.78 (d, 1H). ^{13}C NMR δ (CD_2Cl_2): 170.74, 152.84, 152.72, 152.60, 148.20, 148.19, 147.95, 147.89, 143.23, 143.19, 137.17, 134.50, 134.49, 133.69, 131.20, 130.47, 128.47, 128.44, 127.00, 126.61, 126.58, 126.55, 65.86, 50.31. UV/vis: $\lambda_{max}(CH_3CN)$ = 235 nm, 275, 413, and 444 nm. HR−FAB MS: Theoretical calculated for $[C_{43}H_{28}N_8F_6PRu]^+$, 903.1134; found, 903.1122.

ROMP of Complex 4. [(H_2IMes)(3-Br-py)$_2$(Cl)$_2$Ru=CHPh] (18 mg, 0.02 mmol) was dissolved in 2 mL of dry dichloromethane in a vial equipped with a magnetic stirring bar. After being stirred for a few minutes, this mixture was added dropwise to a solution of complex **4** (42 mg, 0.04 mmol, 2 equiv) in 3 mL of dichloromethane and stirred at room temperature for 12 h. The reaction was quenched by the addition of ethyl vinyl ether (0.5 mL), and the solution was stirred for 30 min. Precipitation in hexanes yielded a dark brown solid, which was filtered and dried in a vacuum. The solid was then loaded on a size-exclusion chromatography column (BioBeads SX-1) and eluted with a 1:1 mixture of CH_3CN and toluene. The collected band was concentrated under vacuum and precipitated in diethyl ether to afford a dark brown solid (oligomer **5**), which was filtered, washed with ether, and dried under vacuum. MALDI-TOF MS: 2199.25 [**5** (n = 2)], 3265.28 [**5** (n = 3) + H_2O], 3847.80 [**5** (n = 4) − 3PF_6^- − (CH_2 end group)], 5331.50 [**5** (n = 5) − (CH_2 end group)]. ESI-MS: m/z = 595.1 [**5** (n = 2) − 3PF_6 + H_2O]$^{3+}$ and 965.1 [**5** (n = 2) − 2PF_6 + H_2O]$^{2+}$.

Oligomer **5** was further purified by size-exclusion chromatography (BioBeads SX-1) and eluted with a 1:3 mixture of CH_3CN and toluene. The second orange band was collected, and the solvent evaporated to give dimer **6**. ^{1}H NMR δ (CD_2Cl_2): 9.61 (br, 2H), 8.56 (br, 4H), 8.21 (br, 6H), 8.06 (br, 4H), 7.74 (br, 6H), 7.36 (br, 2H, olefinic), 3.80 (br, 2H), 2.4 (br, 2H). MALDI-TOF MS: 1894.64 [**6**− 3 PF_6^-], 2043.06 [**6** − PF_6^- − (CH_2 end group)]. ESI-MS: m/z = 584 (**6** − 3PF_6 − [CH_2 end group])$^{3+}$, 948 (**6** − 2PF_6 − [CH_2])$^{2+}$ and 966 (**6** − 2PF_6 + H_2O)$^{2+}$ UV/vis: λ_{max}(CH_3CN) = 221, 263, 417, and 447.0 nm.

Single-Crystal X-ray Diffraction Characterization of Complex 4. A platelet red crystal of complex **4** (0.18 mm × 0.05 mm × 0.05 mm) was grown by vapor diffusion of ether into a dichloromethane solution of the complex at 4 °C. A crystal was cut and mounted on a Bruker AXS Platform diffractometer equipped with a SMART 2K CCD area detector. Data collection and structure solution parameters are listed in Table 1. The initial unit cell parameters were obtained from least-squares refinement by using the setting angles of 1552 reflections in the range θ = 3.14−37.75 ° and correspond to a triclinic cell with dimensions a = 13.0038(15) Å, b = 13.2857(15) Å, and c = 14.8838 Å and β = 91.374(4)°.[4] On the basis of systematic absences, the space group was confirmed by the XPREP routine in the program SHELXTL to be P1. The data were collected at 220 °K. Data reduction processing was carried out by the program SAINT, which applied Lorentz and polarization corrections to three-dimensionally integrated diffraction spots. The program SADBS was utilized for the scaling of diffraction data, the application of a decay correction, and an empirical absorption correction based on redundant reflections. The structure was solved by direct methods using SHELXS-97 and difmap synthesis using SHELXL-96. All non-hydrogen atoms were refined anisotropically, and the isotropic hydrogen atoms were calculated at idealized positions using a riding model (default) C−H distance of 0.93 Å. The isotropic displacement factors, U(iso), were adjusted to a value 20% higher than that of the parent carbon atom for methyl hydrogens.

Acknowledgment. The X-ray structure of complex **4** was solved and refined in the laboratory of X-ray diffraction of the Université de Montréal by Dr. Francine Bélanger Gariépy. The authors gratefully acknowledge Prof. John Harrod for helpful comments and support. A.R. acknowledges financial support from the FQRNT Center for Self-Assembled Chemical Structures. We thank the Natural Sciences and Engineering Research Council of Canada (NSERC), the Canada Foundation for Innovation, the Research Corporation, and the NSERC Strategic Grant program for financial support. H.F.S. is a Cottrell Scholar of the Research Corporation.

Supporting Information Available: (i) MALDI-TOF, (ii) ESI-MS, (iii) theoretical isotopic distribution of oligomer **5** (n = 2) and dimer **6**, (iv) ^{1}H NMR spectrum of dimer **6**, (v) crystallographic data of **4** in CIF format. This material is available free of charge via the Internet at http://pubs.acs.org.

IC0498438